

# Feasibility of B-mode Diagnostic Ultrasonic Energy Transfer and Telemetry to a $\text{cm}^2$ Sized Deep-tissue Implant

Biyi Fang, Tao Feng, Mi Zhang and Shantanu Chakrabartty  
Department of Electrical and Computer Engineering  
Michigan State University  
East Lansing, U.S.A.  
{fangbiyi, fengtao, mizhang, shantanu}@egr.msu.edu

**Abstract**—While radio-frequency based remote powering and back-telemetry is popular for many of the surface implants, like neural prosthesis or under-the-skin implanted batteries, it is not suitable for implants located deep inside the tissue. In this paper, we investigate the feasibility of using a commercial off-the-shelf (COTS), diagnostic ultrasound technology for delivering energy to a sub- $\text{cm}^2$  sized device implanted at depths more than 10cm away from the tissue surface. Using a COTS 3.5MHz ultrasound scanner we show how the B-mode interrogation protocol can be used to deliver energy to an encapsulated PZT transducer and how the B-mode video sequence can be parsed to retrieve the data from the transducer. In this paper we also discuss the limits of energy transfer at different implantation depths and we also discuss the energy requirements at the implant to achieve robust data transfer.

## I. INTRODUCTION

According to a 2013 national survey, about 25% of the patients who underwent orthopedic surgery reported dissatisfaction with their surgical outcomes [1]. This indicates a major problem since annually about 600,000 joint prostheses and 2,000,000 fracture-fixation devices are surgically implanted in the U.S. [2]. One way to help achieve better orthopedic surgical outcomes is to use advanced sensing technology to continuously monitor the mechanical usage of orthopedic implants post-surgery. In [3] we had reported a self-powered sensor that can continuously monitor the history of mechanical usage of an orthopedic implant by harvesting energy from strain variations at the implantation site. Typically the harvestable power levels from in-vivo strain variations is in nano-watts [4]. Thus while this level of energy is sufficient for energizing basic sensing, computation and storage circuitry, the energy is not sufficient for establishing communication with an external reader. One possible solution is to use radio-frequency (RF) waves to deliver energy to the implant and establish communications with the implant. However, the size of the antenna and high levels of attenuation limit the applicability of RF techniques to orthopedic implant sensors. In Fig. 1, we compare the form-factors and the implantation distances reported for some of the state-of-the-art RF biotelemetry systems [5]-[10]. The comparison clearly shows that the majority of existing RF telemetry systems for orthopedic implant sensors have the limitation that they cannot be located at depths greater than 50mm. Also, many orthopedic implants and fixation devices are made with metal which could lead to significant distortion of impinging RF fields.

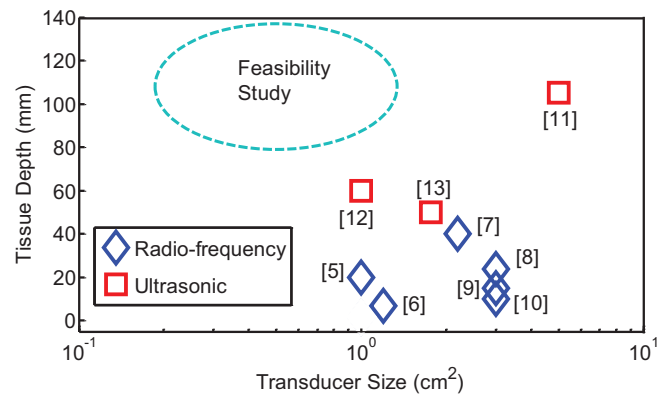


Fig. 1. An overview of current technologies of implantation devices with corresponding receiver size versus implantation depth [5]-[13].

An alternative solution for deep-tissue energy transfer and telemetry is to use ultrasonic waves which have been demonstrated to have lower attenuation inside biological tissue. A piezoelectric material (e.g. PZT, PVDF or Zinc Oxide) can then be used as a transducer for harvesting ultrasonic energy and for transmitting sensor data. In Fig. 1, we also compare the form-factors and implantation depths for different ultrasonic bio-telemetry devices [11]-[13]. While the implantation depths reported in some of these studies could reach distances suitable for orthopedic implants, the sizes of the transducers are relatively large. Also most of these reported results are based on custom-made ultrasonic transceivers and hence it is not clear if they are compliant with medical regulations.

In this paper we investigate the feasibility of using a commercial, medically compliant, diagnostic ultrasound technology for transferring energy and retrieving data from an orthopedic implant sensor. Also, using the diagnostic ultrasound technology we will investigate the trade-off between the the implant (transducer) size and the implantation depth as shown in Fig. 1. Note for the self-powered sensor reported in [3], the data transfer rate is nominal ranging from 1bps to 100bps. It is envisioned that the self-powered sensor will continuously monitor the strain-levels experienced by a trauma fixation device and continuously record the usage statistics. During post-surgical checkup, the surgeon will retrieve the usage data using the diagnostic ultrasound, and the retrieved

data will provide predictive information enabling orthopedic surgeons to plan for any intervention surgery if needed.

## II. B-MODE ULTRASONIC DIAGNOSTIC INSTRUMENTS

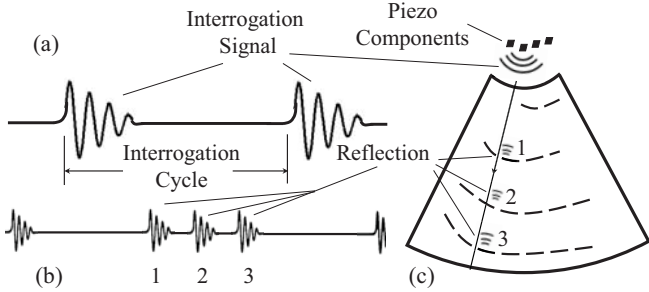


Fig. 2. The principle of operation of a B-mode Ultrasonic Diagnostic Instrument. (a) Interrogation ultrasonic pluses generated by a diagnostic probe. An certain interval of time is waited so that all reflections are collected; (b) Reflection signals from tissue collected by piezoelectric components. Reflection 1 can be ultrasound reflected by the skin, while 2 and 3 can be from fat and bones. (c) An illustration of real-time gray-scale diagnostic image.

The principle of B-mode ultrasonic diagnostic instrument (UDI) is illustrated in Fig. 2. An ultrasonic probe comprising of an array of piezoelectric transducers generates a periodic train of acoustic interrogation pulses as shown in Fig. 2(a). After every interrogation pulse, the ultrasonic probe listens to any echoes of the interrogation pulse (as shown in Fig. 2(b)) that get reflected at boundaries between tissues with different acoustic impedances (as shown in Fig. 2(c)). The strength of the echoes reflect the degree of acoustic impedance mismatch and hence can be used to image and discern tissue boundaries. For instance, stronger echoes are reflected back from denser tissues such as bones, while weaker echoes are reflected from soft tissues such as heart or kidney. Typically for a single transducer, the reflections convey information related tissue boundaries located along one radial axis (or one dimension). However, when an array of piezoelectric transducers is used for interrogation as shown in Fig. 2, the reflections can be used to construct a 2-D image of the tissue. The final B-mode ultrasound image is obtained after applying different image smoothing techniques [14].

## III. EXPERIMENTAL SETUP

The schematic and the image of the experimental setup used in this feasibility study is shown in Fig. 3(a). A RUS-6000D full digital ultrasound scanner, was configured to operate in B-mode and a 3.5MHz convex-array ultrasound probe was used to acquire B-mode video. The scanner was interfaced with a laptop using a USB interface and the real-time video acquired through the USB interface was used to extract the signals of interest.

We have sub-divided our experiments into two categories: (a) the experiment where the implantation depth is varied; and (b) the experiment where the power budget for data transmission is varied.

TABLE I. ACOUSTIC PROPERTY OF TISSUE AND PDMS [15] [16].

Material	Velocity (m/s)	Density (kg/m <sup>3</sup> )	Attenuation (dB/cm MHz)
Air	330	1.2	-
Water	1480	1000	0.0022
Blood	1584	1060	0.2
Muscle	1547	1050	1.09
PDMS (10:1)	1076.5	965	~3.7
Tendon	1670	1100	4.7
Bone, Cortical	3476	1975	6.9
Bone, Trabecular	1886	1055	9.94

### A. Setup to Study Isotropic Power Delivery

The acoustic environment in-vivo is highly complex due to the presence of muscles, blood-flow, tendons, fat, membranes, organs and bones. Thus for signal attenuation studies and to ensure consistency between different experimental runs, it is more useful to use a isotropic, homogeneous material with acoustical properties similar to that of a typical biological tissue. In Table I we summarize the acoustic properties of some of the tissue materials and compare it with the property of Polydimethylsiloxane (PDMS) which has a similar acoustic impedance and is easy to synthesize in the laboratory. Therefore we used PDMS to emulate the biological tissue in human body in our experiment.

The fabrication of a PDMS phantom involved the following steps: The pre-polymer and curing reagent of PDMS were mixed at a ratio of 10:1 (w/w) and then degassed in a vacuum container for about 20 min. The mixture was then poured in a Petri dish with dimensions of 85mm diameter and 6mm height. The was placed in an incubator for 10 minutes and the temperature was set to 75°C. A PZT transducer (with property summarized in Table II) was then placed on the surface of the semi-cured PDMS in the Petri dish, and another portion of the same PDMS mixture was poured on the transducer to encapsulate it. The thickness of the second PDMS layer was chosen to be 7mm. The dish was incubated at 75 °C incubator for another 20 min, after which, the two layers of PDMS fused together to form an encapsulation as shown in Fig. 3(b). Embedding the PZT transducer inside PDMS prevented the introduction of any air pockets and reduced additional acoustic losses. To measure the energy (or power) that can be delivered to the transducer, we connected a 220Ω load at the PZT terminals and measured the voltage across the resistor.

TABLE II. PZT TRANSDUCER PARAMETERS

Paramters	Data
Density (kg/m <sup>2</sup> )	7800
Velocity (m/s)	2820
Thickness (mm)	0.6
Frequency (MHz)	3.4
Area (cm <sup>2</sup> )	1.1

### B. Setup to Study Implant Power Dissipation Requirements

For this study it was assumed that the data transmission at the implant was the dominant source of power dissipation. Therefore, the goal of these sets of experiment was to determine the power required to drive the PZT such that the ultrasound scanner can decode the sensor data. A picture of the setup is shown in Fig. 3(b). We used multiple layers of chicken breast and pork ribs to emulate an in-vivo transmission

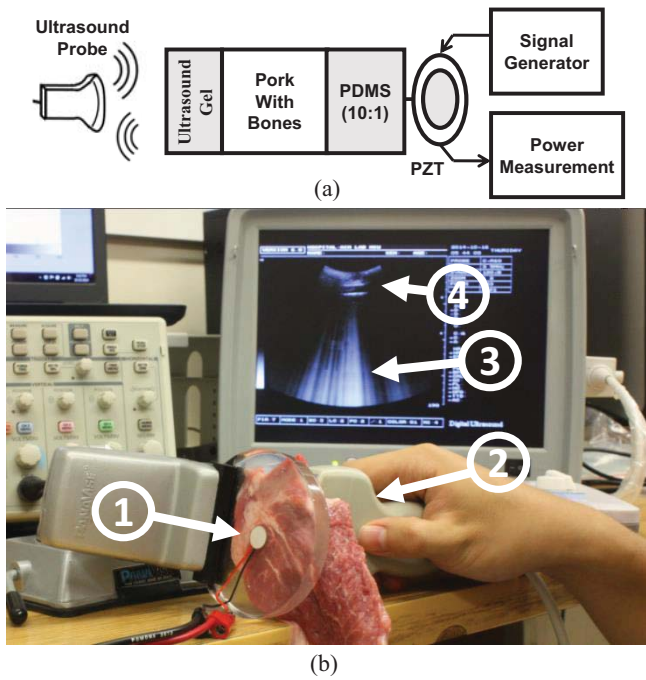


Fig. 3. (a) Image of the experimental setup. 1. PZT disk embedded PDMS ; 2. A convex ultrasonic 3.5MHz probe; 3. Section of the B-mode video showing ultrasonic image of sensor data; 4. Section of the B-mode video showing reflections from the tissue discontinuities within pork; (b) A schematic view of the experimental setup used for energy transfer and telemetry studies.

environment that is at least  $100\text{mm}$  thick. An ultrasonic gel was placed at the surface of the meat to reduce acoustic impedance mismatch between the ultrasonic probe and the tissue. A programmable signal generator was connected to the transducer through a series resistance of  $1\text{K}\Omega$ . The current flowing through the resistor was measured and was used to estimate the average power dissipated through the piezoelectric transducer. The signal source was programmed to generate a 3.5MHz carrier which was modulated using ON-OFF keying (modulation frequency of 1-3Hz) for emulating the sensor data. The gray-scale B-mode video sequences were then acquired from the ultrasound scanner and the video sequences were then parsed to demodulate the sensor data.

#### IV. MEASUREMENT RESULTS

##### A. Power Delivery Measurements

Fig. 4(a) shows the typical oscilloscope trace recorded at the PZT transducer (located  $10\text{mm}$  away) when the ultrasound scanner periodically emits the interrogation pulses. Note that the transducer is embedded inside PDMS as shown in the schematic in Fig. 3(b). The oscilloscope trace clearly shows bursts of energy that can be delivered at intervals of approximate  $125\mu\text{s}$  which equals the interrogation cycle of the B-mode UDI. For each of these interrogation pulses (shown in Fig. 4(b)), the peak voltage recorded was  $5.7\text{V}$  at a load of  $10\text{M}\Omega$  and the duration of the pulse was measured to be  $5\mu\text{s}$ . It can be envisioned any circuit harvesting energy from the B-mode UDI will buffer energy across multiple interrogation pulses. Using a power measurement setup described in section III, we then estimated the average power that can be delivered to the transducer as a function of the

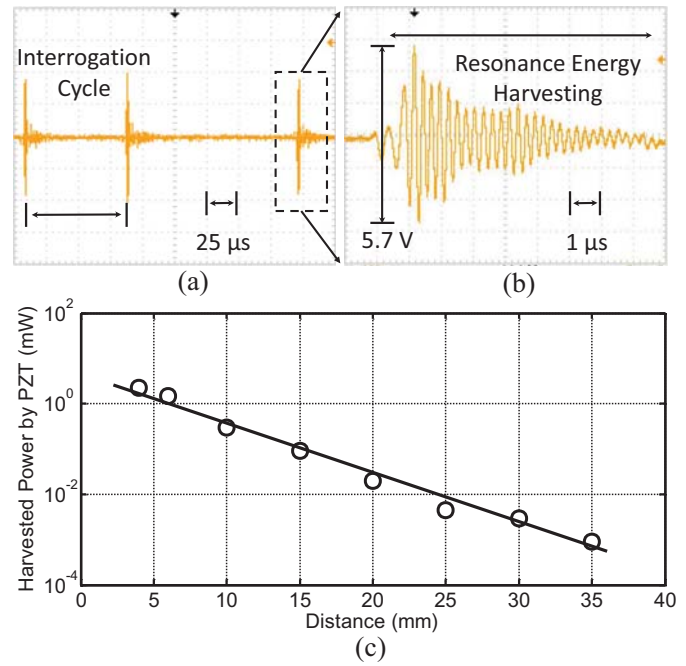


Fig. 4. Measured results showing energy that can be delivered to the transducer using a diagnostic ultrasound: (a) Interrogation pulses measured at the transducer with a load of  $10\text{M}\Omega$ ; (b) Shape of the interrogation pulse showing a resonant response at 3.5MHz; (c) Measured average power levels that can be delivered to the transducer embedded inside PDMS of different thicknesses.

implantation depth. The results are summarized in Fig. 4 which clearly shows the attenuation (less power delivered) as the depth is increased. However, note that this experiment was conducted by varying the thickness of the PDMS material and as we pointed out in section III, this represents the worst-case scenario for ultrasound propagation inside biological tissue.

##### B. Interrogation Results

Fig. 5 shows the measurement data at the UDI when the transducer is driven by a programmable signal generator as shown in Fig. 3(a). The transducer was driven by a 3.5MHz carrier signal which was modulated using ON-OFF keying. The effect of the modulation can be clearly seen by the changes in intensity in the B-mode images as shown in Fig. 5 (a) and (b) during the OFF and ON phases of the modulation cycle. The ultrasound videos were post-processed by cropping the effective region from the original UDI gray-scale image. The 8-bit intensity levels for all pixels in the cropped region were averaged and the result was plotted as a function of the video frames as shown in Fig. 5(c). When the average power dissipation measured at the transducer is  $1\text{mW}$ , the modulation (or the sensor data) can be easily decoded. When the power dissipation at the transducer is reduced to  $10\mu\text{W}$ , the intensity levels in the images and the amplitude of the decoded signal also reduces as shown in Fig. 5(d)(e) and (f). In fact we can reduce the power levels to less than  $1\mu\text{W}$  and still be able to decode the sensor data at interrogation distances greater than  $100\text{mm}$ . If the experiment is repeated with only PDMS (without the meat), we have found that the power dissipation requirements can be reduced to  $55\text{nW}$  for  $10\text{mm}$  thick PDMS.

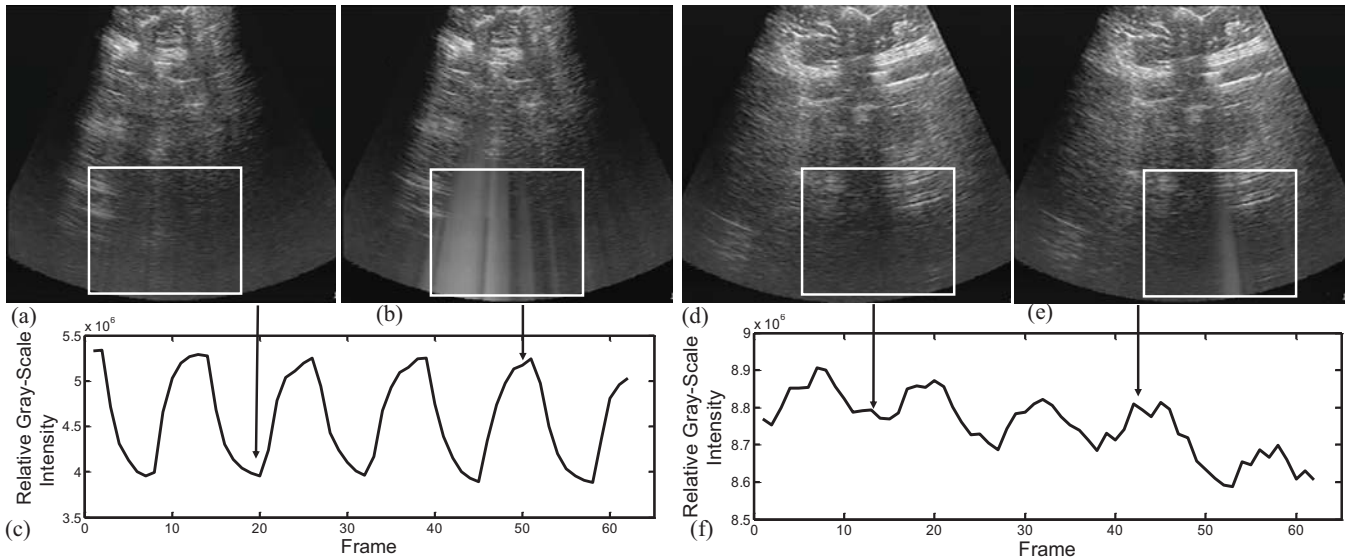


Fig. 5. Measured results showing sensor data received by the ultrasound scanner for two different levels of power dissipation at the sensor: (a) B-mode image during the OFF state of the data modulation cycle ( $1mW$  power dissipation); (b) B-mode image during the ON state of the data modulation cycle ( $1mW$  power dissipation); (c) Demodulated sensor data obtained after parsing the grey-scale ultrasound video ( $1mW$  power dissipation); (d)(e)(f) results obtained when the power dissipation at the sensor is  $10\mu W$ ;

## V. CONCLUSIONS

In this work, we investigated and demonstrated the feasibility of remotely powering and interrogating a  $cm^2$  sized sensor that is implanted at depths greater than  $100mm$  using a COTS diagnostic ultrasound transducer. Our study reveals that the use of ultrasound allows miniaturization of the size of sensor by relaxing the size requirements on the piezoelectric transducer. Also, the plethora of commercial COTS and FDA approved diagnostic ultrasonic imaging instrumentation will make the ultrasonic interrogation of implanted and low data-rate sensors more acceptable to medical practitioners. Future work in this area will involve design of the integrated circuit that can harvest energy from the periodic interrogation pulses, store the energy and then transmit the sensor data back to the UDI when sufficient energy has been buffered. However, the results shown in this paper demonstrate that this is feasible since the energy requirements for low data transmission rates are nominal.

## VI. ACKNOWLEDGEMENT

The authors want to thank Chengpeng Chen of Spence Lab at Michigan State University for the experiment setup.

## REFERENCES

- [1] M. T. Hirschmann, E. Testa, F. Amsler, and N. F. Friederich, "The Unhappy Total knee arthroplasty (TKA) patient: higher womac and lower kss in depressed patients prior and after TKA," *Knee Surgery, Sports Traumatology, Arthroscopy*, vol. 21, no. 10, pp. 2405–2411, 2013.
- [2] S. Kurtz, K. Ong, E. Lau, F. Mowat, and M. Halpern, "Projections of primary and revision hip and knee arthroplasty in the united states from 2005 to 2030," *The Journal of Bone & Joint Surgery*, vol. 89, no. 4, pp. 780–785, 2007.
- [3] S. Chakrabarty, "Self-powered Strain-rate Sensor," Jul. 20 2010, uS Patent 7,757,565.
- [4] G. Research, "The future of orthopedic implants, analysis and forecasts to 2016 - joint reconstruction and spinal implants creating growth opportunities," 2013.

- [5] M. Kiani and M. Ghovanloo, "An rfid-based closed-loop wireless power transmission system for biomedical applications," *Circuits and Systems II: Express Briefs, IEEE Transactions*, vol. 57, no. 4, pp. 260–264, 2010.
- [6] M. Kiani, K. Y. Kwon, F. Zhang, K. Oweiss, and M. Ghovanloo, "Evaluation of a closed loop inductive power transmission system on an awake behaving animal subject," in *Engineering in Medicine and Biology Society, EMBC, 2011 Annual International Conference of the IEEE*. IEEE, 2011, pp. 7658–7661.
- [7] R. Lodato, V. Lopresto, G. Marrocco, and R. Pinto, "Numerical and Experimental Characterization of Through-the-Body UHF-RFID Links for Passive Tags Implanted into Human Limbs," vol. 62, no. 10, pp. 5298–5306, 2014.
- [8] X. Liu, J. L. Berger, A. Ogirala, and M. H. Mickle, "A touch probe method of operating an implantable rfid tag for orthopedic implant identification," *Biomedical Circuits and Systems, IEEE Transactions on*, vol. 7, no. 3, pp. 236–242, 2013.
- [9] C. Occhiuzzi, G. Contri, and G. Marrocco, "Design of implanted rfid tags for passive sensing of human body: the stentag," *Antennas and Propagation, IEEE Transactions on*, vol. 60, no. 7, pp. 3146–3154, 2012.
- [10] X. Liu, R. Yalamanchili, A. Ogirala, and M. Mickle, "An alternative approach of operating a passive rfid device embedded on metallic implants," in *Wireless and Microwave Technology Conference (WAMICON), 2011 IEEE 12th Annual*. IEEE, 2011, pp. 1–6.
- [11] S. Arra, et al, "Ultrasonic power and data link for wireless implantable applications," in *Wireless Pervasive Computing, 2007. ISWPC'07. 2nd International Symposium on*. IEEE, 2007.
- [12] P.-J. Shih and W.-P. Shih, "Design, fabrication, and application of bio-implantable acoustic power transmission," *Microelectromechanical Systems, Journal of*, vol. 19, no. 3, pp. 494–502, 2010.
- [13] S. Ozeri and D. Shmilovitz, "Ultrasonic transcutaneous energy transfer for powering implanted devices," *Ultrasonics*, vol. 50, no. 6, pp. 556–566, 2010.
- [14] R. L. Popp and A. Macovski, "Ultrasonic diagnostic instruments," *Science*, vol. 210, no. 4467, pp. 268–273, 1980.
- [15] J. K. Tsou, et al, "Role of ultrasonic shear rate estimation errors in assessing inflammatory response and vascular risk," *Ultrasound in medicine & biology*, vol. 34, no. 6, pp. 963–972, 2008.
- [16] M. O. Culjat, D. Goldenberg, P. Tewari, and R. S. Singh, "A review of tissue substitutes for ultrasound imaging," *Ultrasound in medicine & biology*, vol. 36, no. 6, pp. 861–873, 2010.